



Experimental Investigation of the Spontaneous Combustion of H2 as a Function of the Temperature in a Hydrogen-fueled Supersonic Combustor

Vilma MAURO¹, Pedro Antonio De Souza MATOS², Leda Marise VIALTA³, Luiz Gilberto BARRETA⁴, Dermeval CARINHANA JR5, Lucas GALEMBECK6

Abstract

The minimum total temperature required to sustain a supersonic combustion was investigated in a hydrogen-fueled supersonic combustor directly connected to a shock tunnel facility. The combustor model comprises an isolator (initial constant area section), followed by a single-hole fuel injection point, a flame-holder cavity and an expansion ramp. In order to find the minimum temperature that provides the spontaneous and stable combustion of H₂ during the test time, dynamic pressure transducers were installed along the combustor model and a high-speed OH* chemiluminescence emission technique was employed to verify the occurrence of supersonic hydrogen combustion. Total temperatures roughly between 750 and 970 K were reached, a range compatible with the ignition temperature of H₂ for hypersonic flows. This configuration led to total pressures of 1.8 to 3.1 MPa. During the experiments, the value of 0.17 ± 0.03 of global equivalence ratio (ϕ) was obtained. The experimental results showed that a stable and spontaneous combustion of H₂ occurs with total temperatures greater than 950 K, during the test time.

Keywords: supersonic combustion, scramjet combustor, spontaneous combustion, minimum temperature, hypersonic shock tunnel

Nomenclature

Latin

A - Area

m - Mass flow

P – Pressure

R - Gas constant T - Temperature

U - Velocity

y - Ratio of specific heats

φ - Equivalence ratio

Subscripts

G - Global

i - Injection

p - Related to the plenum

S - Related to the free-stream

0 - Related to the total conditions

1 - Related to the driven

4 - Related to the driver

1. Introduction

Over the past decades, significant efforts have been devoted to advancing supersonic combustion ramjet (SCRamjet) engines, given their critical role in hypersonic propulsion systems [1]. A central

HiSST-2025-XXXX Experimental Investigation of the Spontaneous Combustion of H2 as a Function of the Temperature in a Hydrogen-fueled Supersonic Combustor Copyright © 2025 by author(s) Commenté [DCJ1]: Verificar pontuação decimal em todo o

Commenté [V2R1]: Feito.

¹ Institute for Advanced Studies, São José dos Campos, Brazil, vilmavm@fab.mil.br

² Institute for Advanced Studies, São José dos Campos, Brazil, bolsa28@fab.mil.br

³ Institute for Advanced Studies, São José dos Campos, Brazil, bolsa20@fab.mil.br

⁴ Institute for Advanced Studies, São José dos Campos, Brazil, bolsa22@fab.mil.br ⁵ Institute for Advanced Studies, São José dos Campos, Brazil, dermevaldcj@fab.mil.br

⁶ Institute for Advanced Studies, São José dos Campos, Brazil, galembeckig@fab.mil.br

challenge in SCRamjet development lies in achieving efficient mixing and stable combustion in the short residence time imposed by supersonic flow conditions [2]. Flameholders, particularly wall cavities, have shown promising results by enhancing fuel-air mixing and anchoring the flame with minimal pressure losses [3-5]. The geometry of such cavities and the injection configuration play a decisive role in shaping the recirculation zones and shear layers that govern ignition and combustion stability [6].

Among the key parameters affecting supersonic combustion are the global equivalence ratio and the pressure conditions of fuel injection [7]. These factors directly influence turbulence intensity, mixing times, and flame propagation characteristics. Variations in fuel injection pressure alter the fuel/oxidizer distribution, which impacts the reaction rates and, ultimately, combustion efficiency. Understanding how these parameters interact under high-speed flow conditions is essential for optimizing engine performance and expanding the operability range of hypersonic vehicles [2,8].

This study builds upon previous experimental campaigns conducted in the T1 shock tunnel facility, which explored various combustion chamber configurations. In this work, we map the operating limits of supersonic combustion by varying the driver—driven pressure ratio and determining the minimum conditions, as pressure, temperature and equivalence ratio that yield hydrogen autoignition during the available test time. Although the present study focuses on the total temperature (T₀), it extends and updates the findings reported in earlier studies [9–11]. Details regarding the facility, experimental methodology, and diagnostic techniques are presented in the subsequent sections.

1.1. T1 shock tunnel facility

The T1 shock tunnel facility is located at the Hypersonic and Aerothermodynamics Laboratory (LAH) at the Institute of Advanced Studies (IEAv), of the Department of Aerospace Science and Technology (DCTA), in São José dos Campos, Brazil.

Structurally, the T1 shock tunnel is basically composed of the shock tube and the combustor. The shock tube consists of a high-pressure section called "driver", filled to an initial pressure known as P_4 , and a low-pressure section called the "driven", filled with the test gas of interest at pressure P_1 . The combustor is composed of the shock tunnel nozzle and the test section, which include the combustion chamber and the injection system. This configuration described is illustrated in Fig. 1.

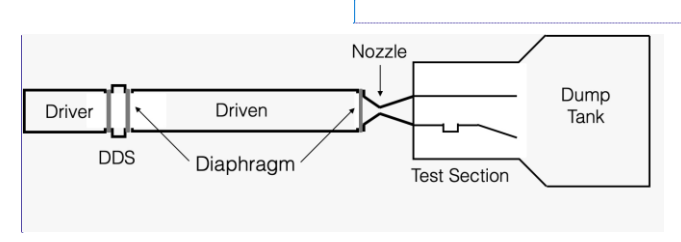


Fig 1. Schematic of the T1 shock tunnel facility configuration, including Driver, Driven, nozzle, test section and dump tank.

In terms of operation, the T1 shock tunnel uses a direct-connect testing mode, that is, the convergent-divergent nozzle outlet is directly connected to the end of the Driven section (or to the model inlet), accelerating the flow to supersonic speeds at the combustor entrance. Further deeper details about this shock tunnel facility and its operation for supersonic testing can be found in the references [9-12].

1.2. Total pressure (P₀), total temperature (T₀) and global equivalence ratio (φ)

From a practical standpoint, when the incident shock wave reaches the end wall of the shock tube, it reflects and travels back, further increasing the gas pressure. The region between the end wall and the reflected shock wave, where the gas reaches high temperature and pressure, referred to as T_0 and P_0 , respectively, is known as the stagnation or reservoir region [9,13].

Commenté [DCJ3]: Variar a razão P4/P1 foi o meio (ferramenta) de se variar as condições no interior do combustor. Dê ênfase nessas condições. A razão de pressões entra na metodologia.

Commenté [V4R3]: Reescrito.

Commenté [DCJ5]: Esse não é o esquema atual de funcionamento do T1, pois o combustor está no modo diretamente conectado. Veja as teses da leda e do Schiavinat

Commenté [V6R5]: Desenho refeito.

ommenté [DCJ7]: Esse item, também conceitual, pode se

Commenté [V8R7]: Reescrito.

Copyright © 2025 by author(s)

HiSST-2025-XXXX Page 2

Author A. First, Author B. Second

This high parameters in the reservoir ruptures the end-wall diaphragm, allowing the high-enthalpy gas to flow through the convergent-divergent nozzle. The flow accelerates from rest to sonic velocity at the throat, then continues to accelerate to supersonic speeds as it moves toward the model [9].

For the continued progress in understanding supersonic combustion, it is essential to clarify how fuel injection, mixing, self-ignition and combustion characteristics are influenced by external parameters, such as global equivalence ratio. So, varying the equivalence ratio values, we can better quantify these effects [7,11].

1.3. Spectral signature of the OH* radical

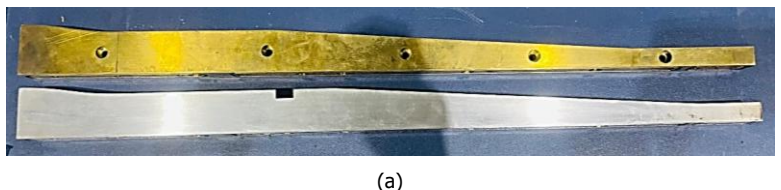
The release of combustion energy through light emission enables the use of cameras for non-intrusive diagnostics. In the combustion between hydrogen and oxygen, the most common intermediate products are water and hydroxyl (OH*). Therefore, a non-intrusive diagnostic technique known as the spectral signature of the OH* radical technique allowed the detection of combustion occurrence within the models, using the emission of the OH* radical [10].

A preliminary literature review revealed no reports of a quantitative analysis of this type that, for each established test condition, applies a binary classification (burn/no-burn) and evaluates whether flame stabilization occurs during combustion. Therefore, the OH radical spectral signature technique was employed to construct a classification map aimed at identifying the combustion zone, using stagnation or total temperature (T_0) as the independent variable.

2. Material and Methods

2.1. Supersonic combustor machining

The combustor used was manufactured at the Institute for Advanced Studies, with the upper section made of a copper–zinc metal alloy and the lower section made of aluminum, as demonstrated at Fig. 2 (a). A Mach 2.7 flow was established at the isolator region by the nozzle. The combustion chamber includes a 1.9 mm diameter orifice for transversal injection of molecular hydrogen (H₂), indicated as T.I. in Fig. 2, a cavity measuring 20 mm in width and 10 mm in height and a 4° inclined expansion ramp at the downstream end. The model was designed to accommodate 14 pressure transducers, as numbered 1-14 in the design presented in Fig. 2. (b) [10-12].



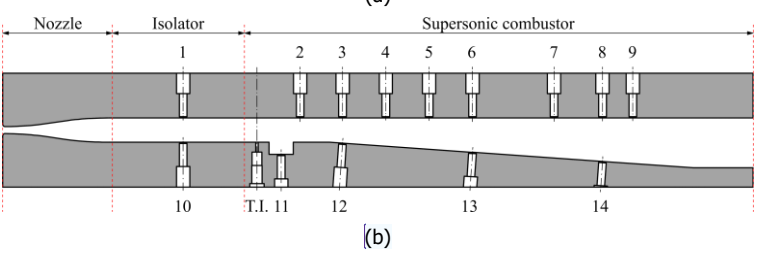


Fig 2. Experimental model: (a) Manufactured combustor (b) model design, including nozzle, isolator, supersonic combustor regions, distribution of 1-9 upper wall sensors and 10-14 lower wall sensors.

Commenté [DCJ9]: Não entendi a expressão "classificação binária".

Commenté [V10R9]: Reescrito.

Commenté [DCJ11]: Identifique na fig 2

Commenté [V12R11]: Feito.

Commenté [DCJ13]: Acrescente: numerados de 1 a 14 na fig 2.

Commenté [V14R13]: Feito.

Commenté [DCJ15]: Acrescente na legenda uma lista atribuindo os números observados no esquema. Ex: 1-9 sensores de cima, 10 a 14, sensores de baixo.

Commenté [V16R15]: Feito.

2.2. Dynamic pressure transducers, signal acquisition and pressure measurements

In this paper, 24 valid experiments were conducted in the T1 shock tunnel facility. The combustor geometry was kept constant and the driver/driven fill conditions were varied across runs. Once the value of P4 was fixed (4.5 MPa for 11 experiments and 5.0 MPa for the rest), only the initial driven-section pressure P₁ was varied, from 110 to 140 kPa.

Regarding the pressure measurements, the data acquisition system used in the experiments consisted of a signal conditioner and oscilloscopes, as illustrated in the schematic shown in Fig. 3. In summary, all pressure transducers are connected to a signal conditioner, which is connected to an oscilloscope.

All pressure transducers used have a known sensitivity (a proportionality constant between the output voltage and the measured pressure) expressed in voltage per unit of pressure. To obtain the pressure values, the measured voltage signals were converted by dividing them by the corresponding sensor sensitivities. Therefore, the signals recorded from all pressure transducers are proportional to voltage outputs.

Following previous studies [9,12], the useful test time for this work was the most stable segment of the plateau in the P5 transducer signal, corresponding to a 500 µs interval. The measured stagnation pressure for each experiment was defined as the average of all measurements within the interval comprised by the test time previously defined. The mean pressure over this interval was obtained using the Yokogawa Xviewer [17], with standard deviation of 4%.

The temperature values were calculated by an iterative process reported in a previous study [15], involving a practical method for atmospheric air, used to incorporate the properties of air in equilibrium and at high temperatures into flow equation calculations, through a polynomial correlation process between tabulated and calculated data [13-15]. The Shock Tube and Tunnel Calculator [16] was used to estimate the real flow conditions generated, as applied in previous works from the same research line [9-12]. The parameters for calculation were the driven pressure and temperature (P_1 and T_1), the primary shock speed (Us) and the area ratio of nozzle exit. The shocked and reflected conditions are computed by treating the gas as equilibrium air that is successively processed by a normal incident shock and its normal reflection. The reflected-shock strength is assumed so that the post-reflection flow is brought to rest. When the reservoir pressure (P_0) is specified, the reservoir (stagnation) state from the reflected-shock state is estimated by assuming an isentropic transformation [13,16].

2.3. Global Equivalence Ratio (φ)

The experimental model corresponds to a supersonic combustor with a simplified geometry, dimensionally comparable to the final design of the 14-XS technological demonstrator [9-10]. As previously mentioned, the T1 facility is directly connected to this combustion chamber for supersonic combustion studies.

The injection of H₂ was initiated by a fast-acting valve, as described in [11]. A pressure transducer positioned in the plenum upstream of the injection orifice was used to monitor both the injection pressure (P_p) and the hydrogen mass flow rate (\dot{m}_{H2}) [11]. The relation between plenum pressure and fuel mass flow rate is demonstrated in Eq. 1.

$$\dot{m}_{H2} \! = \! A_i \frac{P_p}{\sqrt{T_p}} \sqrt{\frac{Y}{R} \left(\frac{2}{\gamma+1}\right)^{\frac{\gamma+1}{\gamma+1}}} \tag{1}$$

Copyright © 2025 by author(s)

in which Ai, Tp, γ and R mean the injection orifice area, the room temperature, the ratio of specific heats and the gas constant for molecular hydrogen, respectively [11].

The air mass flow rate was calculated similarly using Eq. 1, by using Po, To and Yo as total pressure, temperature and specific heat ratio data.

So, considering the air mass flow rate (\dot{m}_{air}) in the experiments, a global equivalence ration is defined by the Eq. 2 [3]:

HiSST-2025-XXXX Author A. First, Author B. Second Commenté [DCJ17]: Melhore (ou retire) a tabela. Não Explique, na forma de texto, que P4 foi variado de 4,5 e 5, e P1, 110, 120 130 e 140. Quantos experimentos foram para

Commenté [V18R17]: Tabela removida.

Commenté [DCJ19]: Isso já foi explicado na Fig. 2. A Fig 3 pode ser retirada, mesmo po está uma verdadeira receita para se fazer um túnel hipersônico.

Commenté [V20R19]: Feito.

Commenté [DCJ21]: Essa informação é relevante? Não seria mesmo que dizer que o líquido de um termômetro se

Commenté [V22R21]: Optei por permanecer com o texto, mas ainda pode ser retirado, a seu critério.

Commenté [DCJ23]: Esse dado talvez seja importante mostrar. Retirar a menção ao siftware, pois podemos usar até

Commenté [V24R23]: Melhorei o texto.

Commenté [DCJ251: Isso é metodolo

Commenté [V26R25]: Trazido para metodologia.

Commenté [DCJ27]: Esse dado é relevante. Não pega bem

Commenté [V28R27]: Dermeval, aqui confirmei com o Giba/Pedrão, o método iterativo está explicado na ref. do Sala [15] e já é bem estabelecido. Nos trabalhos sempre somente falamos que é um método completo, numérico, e dispensamos o detalhamento de equações no texto, até mesmo porque é multi-iterativo complexo e possui relações empíricas muito

Commenté [DCJ29]: Tem que explicar melhor. Onde ele

Commenté [V30R29]: Indicado na Fig. 2.

Commenté [DCJ31]: P é maiúsculo ou minúsculo? Na

Commenté [V32R31]: Corrigido.

Commenté [DCJ33]: Isso é metodologia. Nesse item, deve ser explicado somente o conceito de Equivalência Global.

Commenté [V34R33]: Feito.

Commenté [DCJ35]: Esse conceito só é explicado no item

Commenté [V36R35]: Alterado conforme sugestões.

$$\varphi_G = 34,48 \frac{\dot{m}_{H2}}{\dot{m}_{air}} \tag{2}$$

Here all calculations and data processing were performed in Microsoft® 365 Excel.

2.4. Non-intrusive diagnostic technique and data processing

For this study, in terms of operation, a Phantom® V1612 high-speed camera, with a resolution of 512 \times 512 pixels and acquisition rate of 10 kHz, was aligned with the combustion chamber to capture the spectral signature of the excited hydroxyl radical (OH*). Also was employed a bandpass filter centered around 306.0 nm to filter, coupled to a Lambert® HiCATT image intensifier (model II 18) to intensify and enhance signal detection.

For analyzing the obtained data, we followed a sequential image-processing workflow comprising definition of the region of interest, extraction and correction of OH* emission intensities and application of a threshold to indicate the occurrence of combustion. The steps are described below:

 Mask definition: the analysis mask was derived from the accumulation of multiple experiments so as to highlight the OH* emission region. This procedure was adopted to mitigate possible camera shifts over the experimental campaign. By restricting the analysis to pixels within this mask, only the relevant image regions are retained, thereby reducing spurious contributions and improving consistency in subsequent analyses.

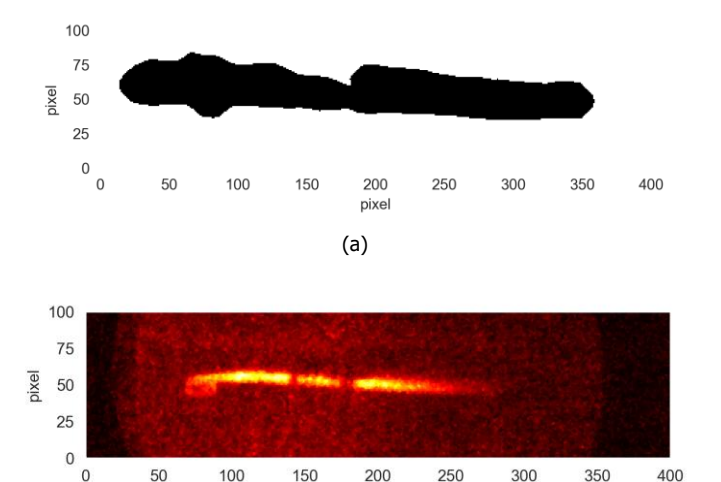


Fig 3. Illustration of the mask (a) and an image collected for frame 7 of experiment number 105

pixel (b)

Intensity definition: each experiment produced a sequence of frames acquired at 10 kHz. All processing was restricted to pixels within the analysis mask. For every frame, the OH* emission intensity was computed by spatially integrating the pixel values under the mask, yielding a frame-indexed time series that tracks the evolution of OH* emission over the course of the

Commenté [DCJ37]: Precisa explicar melhor essa seção, incluindo figuras que ilustrem o processo de determinação das intensidades, do estabelecimento do limiar (threshold), etc.

Commenté [V38R37]: A seção 2.4 e 3.2 foi corrigida/revisada pelo Pedrão.

Commenté [DCJ39]: São duas coisas diferentes: o filtro é para filtrar e o intensificador, é para intensificar!

Commenté [V40R39]: Texto modificado.

Commenté [DCJ41]: Explicar melhor esse processo. Como foi definida a área da máscara? Com que propósito esse procedimento foi realizado?

Commenté [V42R41]: Metodologia revisada pelo Pedrão, passos de 1 a 5, conforme suas anotações/correções.

experiment.

- 3. Background identification: for each experiment, the background intensity was estimated from the integrated intensity of the first frame within the mask, prior to the onset of OH* emission. This value represents the baseline of the optical system, including random fluctuations that affect the image. Background removal ensures that the intensities computed for subsequent frames reflect only the combustion-related OH* emission.
- 4. Background correction: for each experiment, the previously estimated background level was subtracted from the integrated intensity at every frame. The result is a background-corrected intensity time series that represents the evolution of OH* emission free from the system baseline. These vectors were subsequently used to compare against each experiment's total temperature and to define the combustion threshold.
- 5. Combustion-threshold determination: background-corrected intensities from all experiments were normalized by a single global factor to enable consistent comparisons across runs. Based on manual inspection of all images and corresponding time series, a threshold of 0.8 was adopted: combustion is deemed to occur in any frame whose normalized intensity exceeds this value. This threshold balances correct identification of combustion frames against false positives due to noise.

3. Results

3.1. Operating boundary based on temperature

Experiment IDs ranged from 91 to 117. The experiments 102, 103 and 104 were discarded.

After the experiments, the following parameters were achieved in the shock tunnel (Table 1):

Experiments, P₄/P₁ reservoir filling pressure values [kPa], with the respective ranges of P_0 , T_0 and φ achieved

Experiment ID	P ₄ /P ₁ Pressure Ratio	Total Pressure (P_0) [MPa]	Total Temperature (T_0) [K]	Equivalence Ratio (φ _G)
91 to 101	$32 < \frac{P_4}{P_1} < 41$	$1.80 < P_0 < 2.40$ ± 0.10	748 < T ₀ < 887 ± 10	0.13 < φ _G < 0.16
105 to 117	$36 < \frac{F_4}{F_1} < 46$	$ 2.80 < P_0 < 3.10 $ ± 0.12	855 < T ₀ < 964 ± 10	$0.17 < \phi_G < 0.2$ 1

The driver pressure was fixed at $P_4 = 4.5$ MPa for runs 91-101 and at $P_4 = 5.0$ MPa for runs 105-117. Under these conditions, only the initial driven-section pressure P₁ was varied, from 110 to 140 kPa, as described previously, yielding the P4/P1 ratios summarized in Table 1. This configuration produced total pressure values (measured) between 1.8 and 3.1 MPa and total temperatures between 750 and 970 K (Table 1). Such range of temperature is compatible with the operational autoignition temperature of hydrogen for hypersonic flows, which is approximately 1000-1100 K, as reported in reference [18].

The standard deviation of total pressure was computed from sample statistics and of total temperature was estimated by error propagation of the experimental measurements.

Commenté [DCJ43]: Junte com a explicação anterior. Por Commenté [V44R43]: Metodologia revisada pelo Pedrão,

passos de 1 a 5, conforme suas anotações/correções.

Commenté [DCJ45]: Como foi definido?

Commenté [V46R45]: Metodologia revisada pelo Pedrão, passos de 1 a 5, conforme suas anotações/correções.

Commenté [DCJ47]: Esse procedimento de cálculo deve

Commenté [V48R47]: Melhor explicado nos itens 2.2 e 2.3.

Commenté [DCJ49]: Verificar números significativos. Se P4

Commenté [V50R49]: Ok.

Commenté [V52R51]: As faixas estabelecidas foram delimitadas de acordo com os experimentos realizados, os quais foram demonstrados na Fig. 4. No texto que sucede a Tab. 1 foi melhor explicado que se trata somente de um intervalo estipulado com os valores máximos e mínimos. As incertezas foram todas inseridas na Tabela.

Commenté [DCJ53]: Como foi calculado? Deve ser explicado com base nas entalpias de combustão.

Commenté [V54R53]: Reescrito. O conceito de antes não era aplicável ao nosso caso. Mas podemos remover essa informação em roxo!!!

HiSST-2025-XXXX

Author A. First, Author B. Second

Copyright © 2025 by author(s)

Additionally, across this set of experiments, the global equivalence ratio (ϕ_G) ranged from 0.13 to 0.21 for each condition (Table 1), res ulting an average of 0.17 \pm 0.03.

Fig. 4 shows better the total temperature versus total pressure $(T_0 \text{ vs. } P_0)$ for each test condition $-P_4 = 4.5 \text{ MPa}$ (squares) and $P_4 = 5.0 \text{ MPa}$ (triangles). Cases exhibiting burn (flame stabilization, during the test time) are highlighted as red triangles, as confirmed by OH* chemiluminescence, which will be detailed in the subsequent sections.

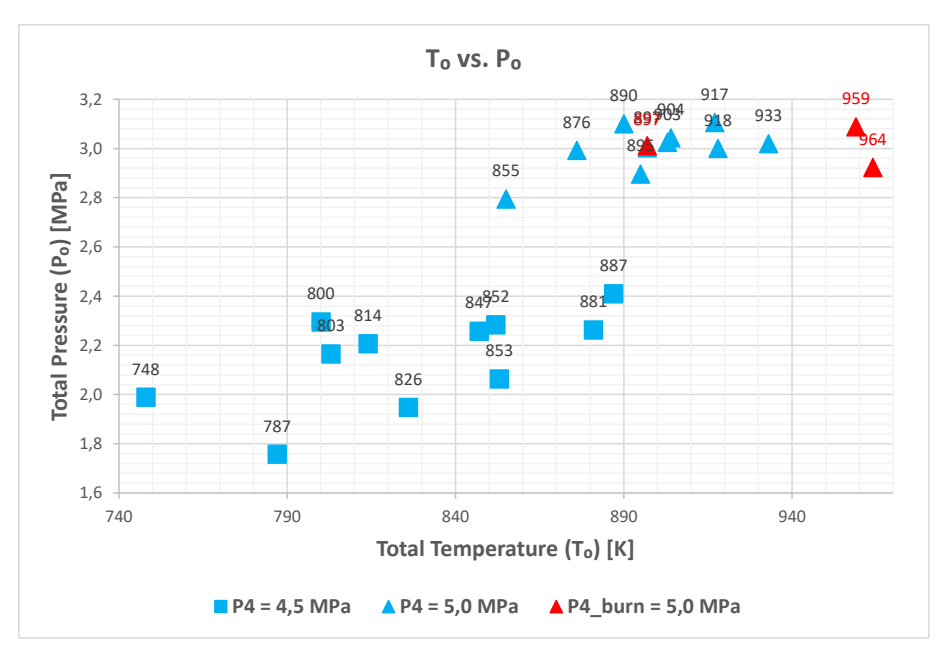


Fig 4. Total temperature (T_0) vs. Total pressure (P_0) plots of the conducted tests: experiments 91 to 117, excluding experiments 102-104.

3.2. OH Radical Spectral Signature Analysis

The results in this section were obtained by applying the image-processing procedure described in Section 2.4.

Fig. 5 shows the OH* emission-intensity profiles as a function of frame number, with the experiments split into two groups for clarity: the first group (IDs 91-101), with a total pressure of about 2 MPa, is shown in Fig. 5 (a); the second group (IDs 105-117), with a total pressure of approximately 3 MPa, is shown in Fig. 5 (b).

For the first group, OH* emission can be identified in the first two frames of each run, even for the case with the lowest total temperature, around 800 K. These emissions, however, are weak, occur upstream of the injector, and were not classified as stable combustion under the method adopted in this study. Hypothetically, premature fuel injection could flood the combustor, transporting H_2 toward the nozzle region near the stagnation point. In that region, the elevated temperature and pressure could favor combustion, and the emission observed in the first two frames would result from interaction with the initially present gas.

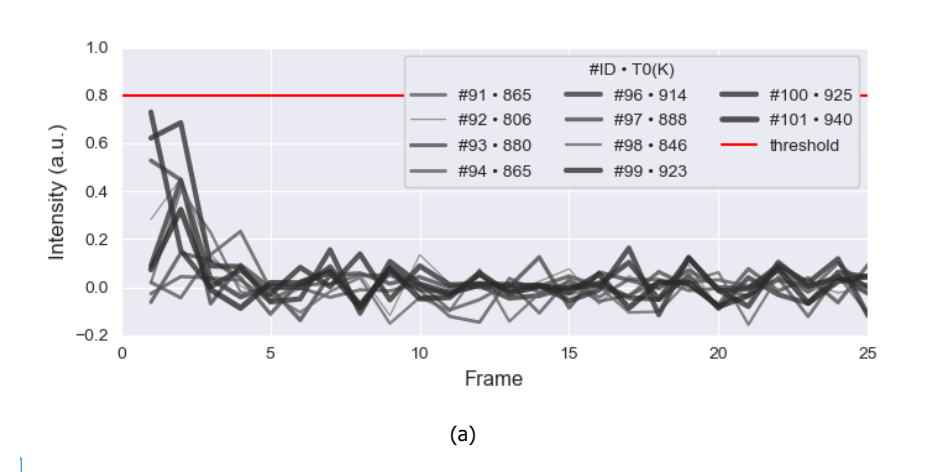
The second group exhibited more complex behavior. In some runs, combustion was detected only in the second frame, whereas in others it persisted at approximately constant intensity for \sim 15 frames.

Commenté [DCJ55]: Os valores de Phi aqui não são estequiométricos, mas foram comparado com o estequiométrico. É isso mesmo?

Commenté [V56R55]: A Eq. 2 descrita no item 2.3 foi utilizada para calcular Phi de cada experimento. Depois tiramos uma média dos valores que resultou em 0.17 ± 0.03 (Phi global).

Commenté [DCJ57]: Qual o critério para ser classificada como estável?

Commenté [V58R57]: Agora isso foi deixado claro em tópicos anteriores. Também foi melhor reescrito aqui.



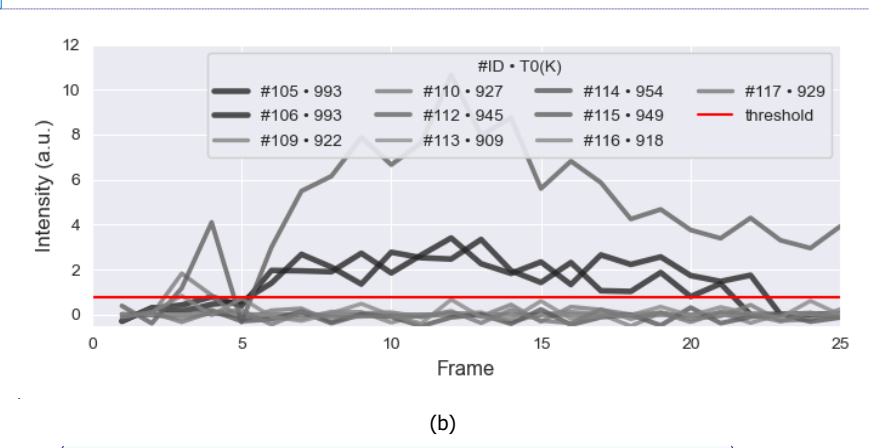


Fig 5. [Intensity vs. Frame plots of the conducted tests: (a) experiments 91 to 101, excluding 95; (b) experiments 105 to 117, excluding 107, 108, and 111.

Based on these results, together with the total temperatures estimated for each experiment, Fig. 6 was constructed. This figure identifies the frames in which combustion occurred and correlates them with the total temperature of each experiment.

As shown in Fig. 6, combustion was not detected in any of the frames corresponding to total temperatures below 890 K. In the intermediate range, between 895 and 940 K, sporadic combustion events were observed, as indicated by the unit markers on the vertical axis. For total temperatures between 950 and 970 K, a more stable combustion regime was achieved, although this conclusion is based on a limited number of test cases.

Commenté [DCJ59]: O que aconteceu com a escala? Tem que ajustar.

Commenté [V60R59]: Escala ajustada.

Commenté [DCJ61]: Ao invés de usar a numeração dos experimentos, explicite a diferença nas condições experimentais entre eles.

Commenté [V62R61]: Optamos por deixar o ID dos

HiSST-2025-XXXX 8 Author A. First, Author B. Second Page I

Copyright © 2025 by author(s)

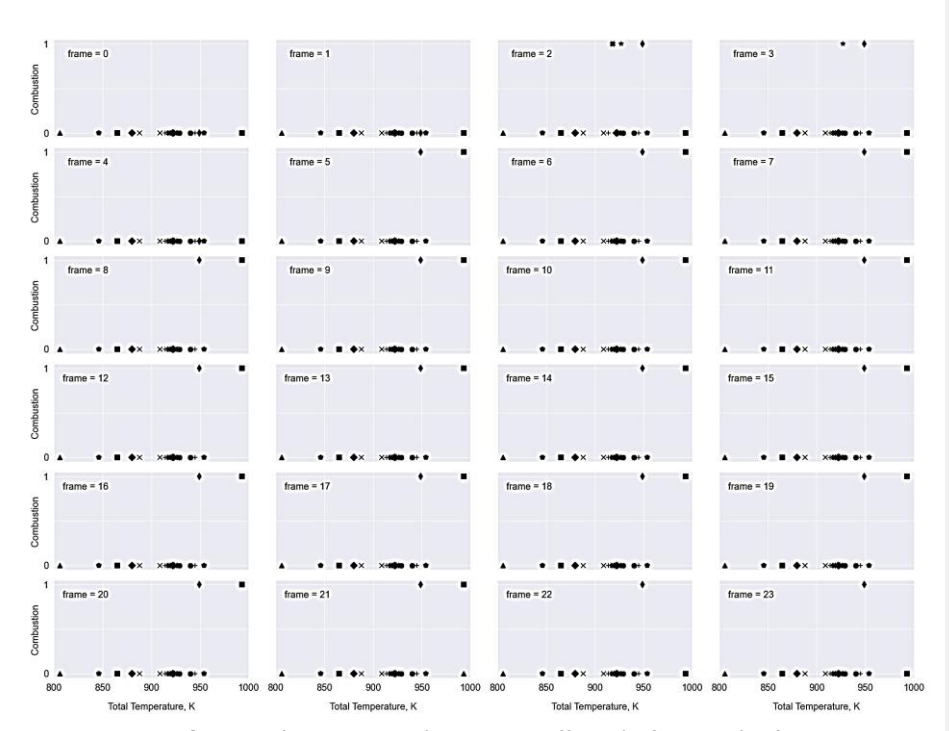


Fig 6. Combustion vs. Total Temperature (frame by frame analysis)

4. Conclusion

Experiments in the T1 Supersonic Shock Tunnel were conducted with the aim of investigating the limits of supersonic combustion. Total temperatures (T_0) ranging from 750 to 970 K were achieved, a range compatible with the ignition temperature of hydrogen for hypersonic flows. This configuration resulted in total pressures (P_0) between 1.8 to 3.1 MPa and the value of 0.17 \pm 0.03 of global equivalence ratio (ϕ_G) was obtained.

In general, it can be stated that experiments conducted at total temperatures between 950 and 970 K led to the combustion stabilization — this condition is confirmed by experiments 105 and 106. This result changes for temperatures between 895 and 940 K, where combustion was occasionally detected, as observed in experiment 115. For temperatures below 890 K, no combustion stabilization was detected — this condition was confirmed by the remaining experiments.

Finally, the experimental results showed that a stable and spontaneous combustion of H₂ during the test time occurs at total temperatures greater than 950 K, corroborated by the OH* chemiluminescence emission technique. This technique was initially employed to construct a classification map capable of identifying the combustion zone, using stagnation temperature as the only independent variable. This procedure represents the first step in a broader effort to apply machine learning for identifying key variables that contribute to stable supersonic combustion.

Further experiments are planned to reach higher T_0 conditions. Ongoing work is mapping and analyzing additional parameters relevant to burn/no-burn identification and to combustion characterization, such as cavity height and width, to provide a more comprehensive assessment.

Commenté [DCJ63]: Vou esperar a nova versão para falar das conclusões.

Commenté [V64R63]: Ok. Foram reescritos alguns pontos.

Acknowledgements

This work was performed within the "Technologies for Hypersonic Flights" project, coordinated by the Institute for Advanced Studies, is supported by the Brazilian Funding Agency for Studies and Projects (FINEP) under the Contract no.: 01.22.0255.00, by the Brazilian Air Force (COMAER) and by the Coordination for the Improvement of Higher Education Personnel (CAPES), under the Contract no.: PROCAD-DEFESA 88881.387753/2019-01. The authors are also grateful to M. A. S Minucci (IEAv) and R. O. Santos (IEAv) for valuable discussion and technical assistance.

References

- $\begin{tabular}{ll} [1] Smart, M.: Scramjets. The Aeronautical Journal 111(1124), $605-619$ (2007). $$ https://doi.org/10.1017/S0001924000004796. $$ \end{tabular}$
- [2] Curran, E.T.: Scramjet engines: the first forty years. Journal of Propulsion and Power, 17(6), 1138-1148 (2001). https://doi.org/10.2514/2.5875.
- [3] Lin, K. C.: Flame characteristics and fuel entrainment inside a cavity flame holder of a scramjet combustor. In 43rd AIAA/ASME/SAE/ASEE joint propulsion conference & exhibit, 5381 (2007). https://doi.org/ 10.2514/6.2007-5381.
- [4] Li, J.: Flame establishment and flameholding modes spontaneous transformation in kerosene axisymmetric supersonic combustor with a plasma igniter. Aerospace Science and Technology, 119, 107080 (2021). https://doi.org/10.1016/j.ast.2021.107080.
- [5] Cisneros-Garibay, E.: Flow and Combustion in a Supersonic Cavity Flameholder. AIAA journal, 60(8), 4566-4577 (2022). https://doi.org/10.2514/1.J061533.
- [6] Cai, Z.: Review of cavity ignition in supersonic flows. Acta Astronautica, 165, 268-286 (2019). https://doi.org/10.1016/j.actaastro.2019.09.016.
- [7] Chapuis, M., et al.: A computational study of the HyShot II combustor performance. Proceedings of the Combustion Institute 34.2 (2013): 2101-2109. http://dx.doi.org/10.1016/j.proci.2012.07.014.
- [8] Wang, Z.: Review of cavity-stabilized combustion for scramjet applications. Proceedings of the Institution of Mechanical Engineers, Part G: Journal of Aerospace Engineering, 228(14), 2718-2735 (2014). https://doi.org/10.1177/0954410014521172.
- [9] Ribeiro, Lucas Alexandre Gonçalves. Semi-empirical study of the air mass flow rate captured by a supersonic combustor. Dissertation of Master of Science. Aeronautics Institute of Technology, Brazil (2022).
- [10] Vialta, L. M. Estudo dos Efeitos de Cavidades Abertas em Combustores Supersônicos. PhD Thesis. Aeronautics Institute of Technology, Brazil (2023).
- [11] Souza, E. S. de; et al. 2024. Experimental Investigation of the Global Equivalence Ratio Influence in a Hydrogen-fueled Supersonic Combustor. In Proceedings of the HiSST: 3rd International Conference on High-Speed Vehicle Science Technology. HiSST, Busan, Korea.
- [12] Souza, E. S. de. Analysis of the Influence of the Global Equivalence Ratio on the Supersonic Combustion of Hydrogen with Atmospheric Air. Dissertation of Master of Science. Aeronautics Institute of Technology, Brazil (2025).
- [13] Anderson Jr., J. D. Fundamentals of Aerodynamics. McGraw-Hill Series in Aeronautical and Aerospace Engineering. 3rd Edition, New York, NY, 2001.
- [14] Tannehill, J. C.; MUGGE, P. H. Improved curve fits for the thermodynamic properties of equilibrium

HiSST-2025-XXXX Page

Author A. First, Author B. Second

air suitable for numerical computation using time dependent or shock-capturing methods, part 1. Washington, DC: NASA, 1974. (NASA-CR-2470).

- [15] Minucci, M. A. S. An experimental investigation of a 2-D scramjet inlet at flow Mach numbers of 8 to 25 and stagnation temperatures of 800 to 4,100 K. 354 p. Thesis (PhD in Aeronatical Engineering) Rensselaer Polytechnic Institute, Troy, NY, 1991.
- [16] Matos, P. A. de S. Shock tube and tunnel caculator. 2020. Android Mobile App. Available at: https://play.google.com/store/apps/details?id=com.pedromatos.stc. Accessed on: 17 April 2022.
- [17] Yokogawa. Xviewer (701992) / XviewerLITE (free software). Alphaville, Barueri, SP: Yokogawa America do Sul, [2008-2025]. Oscilloscopes Application Software.
- [18] Baranyshyn Y.: Ignition Delay and Reaction Time Measurements of Hydrogen–Air Mixtures at High Temperatures. Fire. 2024; 7(2):43. https://doi.org/10.3390/fire7020043

HiSST-2025-XXXX 11 Paper Title